Simultaneous measurement of strain and damage signal of composite structures using a fiber Bragg grating sensor

2005 Smart Mater. Struct. 14 658

(http://iopscience.iop.org/0964-1726/14/4/024)

INSTITUTE OF PHYSICS PUBLISHING SMART MATERIALS AND STRUCTURES
Smart Mater. Struct. **14** (2005) 658–663 doi:10.1088/0964-1726/14/4/024

Simultaneous measurement of strain and damage signal of composite structures using a fiber Bragg grating sensor

Jong-In Koh[1], **Hyung-Joon Bang**[2], **Chun-Gon Kim**[2,3] **and Chang-Sun Hong**[2]

[1] Agency for Defense Development, Daejeon 305-600, Korea
[2] Department of Aerospace Engineering, Korea Advanced Institute of Science and Technology, 373-1, Guseong-dong, Yuseong-gu, Daejeon 305-701, Korea

E-mail: cgkim@kaist.ac.kr

Received 13 April 2004, in final form 7 December 2004
Published 15 June 2005
Online at stacks.iop.org/SMS/14/658

Abstract
For the simultaneous measurement of strain and a damage signal, a fiber Bragg grating sensor system with a dual demodulator is proposed. The dual demodulator is composed of a demodulator with a tunable Fabry–Perot filter measuring the low-frequency signal with large magnitude such as strain and another with a passive Mach–Zehnder interferometer measuring the high-frequency signal with small amplitude such as a damage or impact signal. Using the proposed fiber Bragg grating sensor system, both the strain and the damage signal of a cross-ply laminated composite beam under tensile loading were simultaneously measured. The strain and the damage signal measured by the single fiber Bragg grating sensor showed that sudden strain shifts were accompanied with vibration at a maximum frequency of several hundred kilohertz at the instant of transverse crack propagation in the 90° layer of the composite beam.

(Some figures in this article are in colour only in the electronic version)

1. Introduction

Fiber reinforced composite materials have superior specific stiffness and specific strength over general metals, and their material properties can be tailored to design requirements. At present, they are extensively used in various fields from aerospace engineering to civil engineering, such as in buildings and bridges. Composite materials may have non-uniform material properties dependent on the manufacturing process, and have invisible damage such as delamination, causing compressive strength reduction. Thus, real-time structural health monitoring is required to assess the structural safety of composite materials.

Conventional electrical sensors such as strain gauges, thermocouples, and acoustic emission or piezoelectric sensors, can measure strain, temperature and acoustic emission that are required for structural health monitoring. These sensors have been widely used because they are reliable and economic. However, they can be affected by electromagnetic interference and their lead wire volume becomes larger as the number of sensors increases.

Optical fiber sensors (OFSs), which appeared as the result of the rapid development of electro-optic technologies, are considered to be a promising sensor alternative to the conventional electrical sensors, because they are compact, light-weight, easily embedded in composite structures and immune to electric magnetic interference.

Various types of OFS have been developed. Interferometric sensors such as extrinsic Fabry–Perot interferometer (EFPI) sensors and fiber Bragg grating (FBG) sensors are widely used at present. The interferometric sensors have sufficiently high sensitivity and high-frequency bandwidth to detect acoustic emission. Hence they have been employed for damage detection of composite structures [1, 2].

Commercial FBG sensor systems, which have less sensitivity and less frequency bandwidth but superior multiplexing capability to the interferometric sensors, have

[3] Author to whom any correspondence should be addressed.

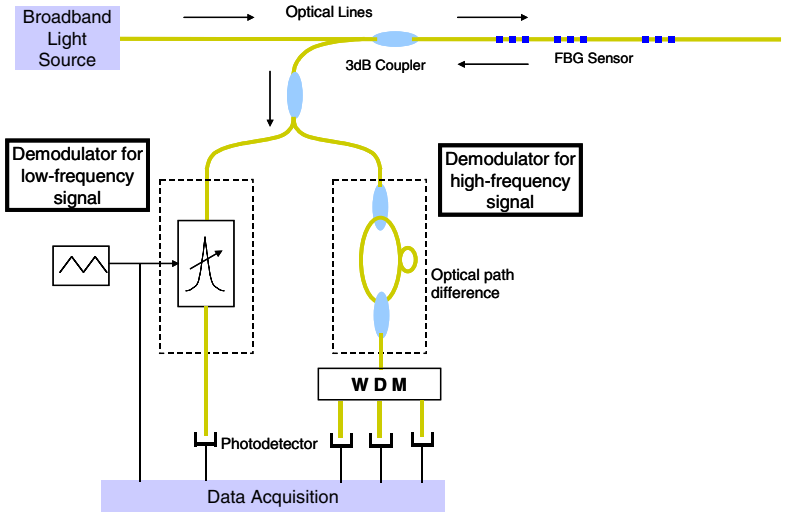

Figure 1. Schematic diagram of an FBG sensor system with a dual demodulator.

been mainly applied to the measurement of quasi-static or low-frequency signals such as strain, temperature and pressure [3, 4]. Recently, the measurements of high-frequency signals such as acoustic emissions have been performed using FBG sensor systems with enhanced sensitivity and frequency bandwidth [5–7]. However, most studies have been focused on the development of demodulators of FBG sensors to increase the sensitivity and bandwidth. A demodulator with enhanced sensitivity and bandwidth can measure the high-frequency signal but the measurement range decreases. So, an FBG sensor system that can measure not only a low-frequency signal with large magnitude such as strain but also a high-frequency signal with small amplitude such as a damage or impact signal will be required for the structural health monitoring of composite structures in the future.

In this paper, the simultaneous measurements of the strain and the damage signal of composite structures were performed using a new FBG sensor system with a dual demodulator. Using a single FBG sensor surface-mounted on a composite beam specimen, both the strain and the damage signals were simultaneously measured during tensile loading and their characteristics were analyzed.

2. New fiber Bragg grating sensor system

2.1. Principles of fiber Bragg grating sensor

An FBG has periodic refractive index changes inscribed in the core of an optical fiber. When broadband light is launched into the FBG, light reflected by the FBG is centered at the Bragg wavelength, λ_B, determined by the Bragg condition given by

$$\lambda_B = 2n_e\Lambda \tag{1}$$

where n_e is the effective refractive index and Λ is the periodicity. When the FBG is disturbed by mechanical strain and temperature change, the shift of the Bragg wavelength, $\Delta\lambda_B$, is expressed as

$$\Delta\lambda_B = \lambda_B\left[(\alpha+\xi)\,\Delta T + (1-p_e)\,\varepsilon\right] \tag{2}$$

where ε is the mechanical strain, ΔT is the temperature change, α is the coefficient of thermal expansion and ξ is the thermo-optic coefficient representing the change of refractive index divided by the change of temperature of the optical fiber. p_e is an effective strain-optic constant and is known to be about 0.22 in a general single mode optical fiber. Without temperature change, the strain is determined from the shift of the Bragg wavelength, and is expressed as

$$\varepsilon = \frac{1}{1-p_e}\frac{\Delta\lambda_B}{\lambda_B}. \tag{3}$$

2.2. Dual demodulator

The demodulation technique that converts the shift of the Bragg wavelength into the physical quantities is very essential in the development of an FBG sensor system, and various demodulation methods have been proposed. At present, a demodulation method using a TFPF (tunable Fabry–Perot filter) [8] is most popular, since it has a wide measurement range and enables easy multiplexing. However, it cannot measure dynamic strain more than several kilohertz due to the limit of wavelength scanning speed. Intensity demodulation mainly using an interferometer that converts the shift of the Bragg wavelength into an intensity variation enables very high measurement speed and high sensitivity, but has a narrow measurement range. For the simultaneous measurement of strain and damage signal, a demodulator with a large measurement range, high bandwidth and high sensitivity is required, but has not yet been developed.

In this paper, an FBG sensor system with a dual demodulator as shown in figure 1 is proposed for the simultaneous measurement of strain and damage signal. The dual demodulator is composed of a demodulator with a TFPF and another with a passive Mach–Zehnder interferometer (MZI). This demodulator has all the advantages of the two types of demodulator, so that one demodulator can measure the low-frequency signal such as strain and the other can measure the high-frequency signal such as the damage or impact signal.

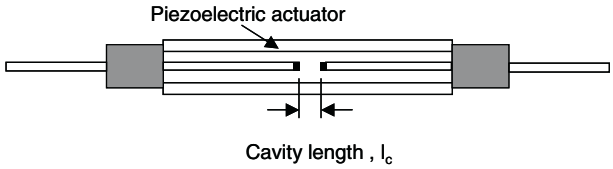

Figure 2. Tunable Fabry–Perot filter.

2.2.1. Demodulation with a tunable Fabry–Perot filter. The TFPF shown in figure 2 can control the cavity length, l_c, so that light transmitted through the TFPF has multiple peak wavelengths given by

$$\lambda_{\text{peak}} = \frac{2nl_c}{N} \tag{4}$$

where n is the refractive index of the cavity and N is integer.

The signal processing algorithm of demodulation with a TFPF is as follows. When voltage with a triangular wave as shown in figure 3 is applied to the TFPF, a piezoelectric actuator changes the cavity length so that the peak wavelength moves. This demodulator measures the reflective Bragg wavelength of the FBG based on the principle that when the peak wavelength of the TFPF is equal to the reflective Bragg wavelength of the FBG, the output voltage of the photodetector detecting the transmitted light through the TFPF becomes the maximum.

In this paper, to measure the absolute reflective wavelength of FBG, two FBGs that could keep constant Bragg wavelengths (λ_{ref1}, λ_{ref2}) by being isolated from exterior environment were used. If it is assumed that the peak wavelength moves linearly with applied voltage, the reflective Bragg wavelength of the FBG sensor, λ_{FBG}, is determined by

$$\lambda_{\text{FBG}} = \lambda_{\text{ref1}} + \frac{(\lambda_{\text{ref2}} - \lambda_{\text{ref1}})}{(t_{\text{ref2}} - t_{\text{ref1}})}(t_{\text{FBG}} - t_{\text{ref1}}) \tag{5}$$

where t_{ref1}, t_{FBG}, t_{ref2} are peak times of the photodetector. The wavelength scanning speed of the TFPF determines the measurement speed of this demodulator.

2.2.2. Demodulation with a passive Mach–Zehnder interferometer. Kersey [9] suggested the Mach–Zehnder interferometric demodulation as a general intensity demodulation method and employed a phase modulator to enhance the linearity and accuracy of the FBG sensor. However, due to the bandwidth limit of the phase modulator, high-frequency signals of more than several tens of kilohertz could not be measured.

In this paper, to detect damage signals that have frequency more than several tens of kilohertz, a passive Mach–Zehnder interferometric demodulator without a phase modulator was employed. Combining two 3 dB fiber optic couplers can easily make a fiber MZI. Interference occurs when the light divided by the first 3 dB coupler passes through a different path length and is combined through the second 3 dB coupler. The ideal transmittance of the MZI is expressed as

$$T = \frac{I_o}{I_i} = \frac{1}{2}\left\{1 + \cos\frac{2\pi nd}{\lambda}\right\} \tag{6}$$

where I_i is the input intensity, I_o is the output intensity, n is the refractive index of the optical fiber, d is the path difference of the interferometer, and λ is the wavelength of light used in the experiment. ϕ is the phase of the interferometer and is defined as

$$\phi = \frac{2\pi nd}{\lambda}. \tag{7}$$

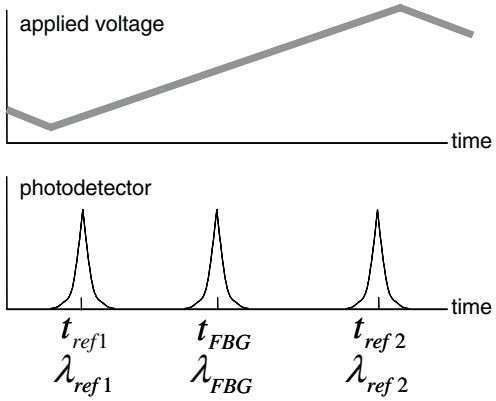

Figure 3. Triangular voltage and output of FBG sensor through a demodulator with a tunable Fabry–Perot filter.

The period of interferometer transmittance is referred to as an FSR (free spectral range) and is expressed in wavelength units as

$$\text{FSR} = \frac{\lambda^2}{nd}. \tag{8}$$

The transmittance of an interferometer is a function of the optical path difference and wavelength. If the optical path difference is constant, the shift of the Bragg wavelength of the FBG sensor is converted into optical power variation through the interferometer. This is the principle of interferometric demodulation of the FBG sensor. Because there is no active device such as a phase modulator, the proposed FBG sensor system needs no additional intermediate signal processing such as phase demodulation. Therefore, it is very simple in configuration and easy to implement, and has a measurement speed up to the photodetector bandwidth generally more than several hundred kilohertz.

The change of transmittance of the interferometer divided by the change of Bragg wavelength represents strain sensitivity, and is dependent upon the phase of the interferometer and the FSR, expressed as

$$\left|\frac{\Delta T}{\Delta\lambda_B}\right| = \left|\sin\left(\frac{2\pi nd}{\lambda_B}\right)\right| \frac{\pi}{\text{FSR}}. \tag{9}$$

In the case of constant phase of the interferometer, as the FSR decreases, the strain sensitivity increases, whereas the strain measurement range decreases and vice versa. Therefore, the FSR should be determined according to the characteristics of the signal to be measured. For example, when a damage signal with small amplitude of strain is to be measured, it is recommended that a small FSR of the interferometer is placed as close to the bandwidth of an FBG sensor as possible to obtain high strain sensitivity of the FBG sensor.

However, the strain sensitivity of a demodulator with a passive MZI is nonlinear except for the quadrature phase, and is not constant along the phases, which need an additional interferometer with quadrature-shifted phase or an active interferometer to hold the output on the optimum point on its transmittance curve.

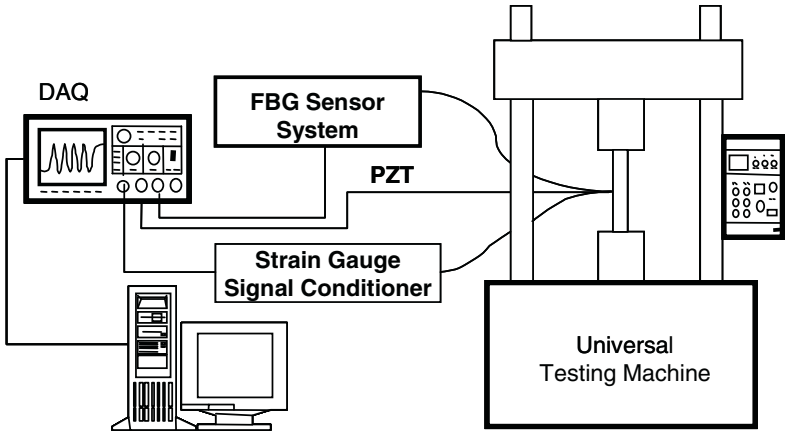

Figure 4. Test setup for the simultaneous measurement of strain and damage signal.

3. Simultaneous measurement of strain and damage signal

Using the proposed FBG sensor system with a dual demodulator, simultaneous measurement of the strain and the damage signal of a composite structure under tensile loading was performed.

3.1. Test setup

The test setup shown in figure 4 is composed of a universal testing machine, a composite specimen, sensors and data acquisition equipment for the sensor output.

The composite specimen was manufactured using graphite/epoxy prepregs (CU-125NS, HFG Co.), which were stacked as $[0_2/90_8]_s$ and cured in an autoclave. The specimen configuration is shown in figure 5, and glass/epoxy taps were attached at both ends of the specimen.

An FBG sensor and a piezoelectric sensor were surface-mounted on one side of the specimen at the center with adhesive bond (cyanoacrylate, TML). An electric strain gauge (ESG) was mounted upon the other side of the specimen at the center. The ESG was connected to a signal conditioner (model P-3500, Vishay) at the 3 dB cut-off frequency of 4 kHz. The piezoelectric sensor (model C-6, Fuji Ceramics) is made of PZT ($Pb(Zi, Ti)O_3$) and is a disk-type of 5 mm in diameter and 2 mm in thickness.

The FBG sensor system is composed of a broadband light source, an FBG sensor, a dual demodulator and photodetectors. The FBG sensor has an initial Bragg wavelength of 1540.5 nm, a gauge length of 10 mm and a bandwidth of about 0.2 nm. The FBG sensor is not recoated after writing since recoating material such as acrylate can affect the high frequency response. The broadband light source (Model BBS1550, JDS Uniphase) has a total optical power of 50 mW and wavelength range of about 40 nm at center wavelength of 1550 nm. A triangular wave with 12 V 200 Hz is applied to the TFPF (Micron Optics) with an FSR of 7150 GHz. Two reference FBGs have reflective Bragg wavelengths of 1536 and 1552 nm. The MZI has an FSR of about 0.8 nm. The output lights of the dual demodulator are detected by two photodetectors (model 2011, NewFocus) at a frequency bandwidth of 200 kHz.

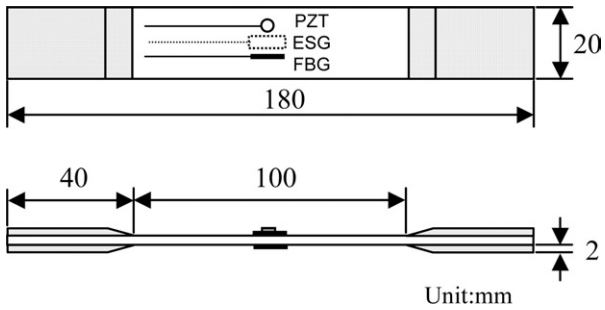

Figure 5. Specimen configuration for the tensile test.

Test procedures including signal processing are as follows.

Tensile load is applied to the composite specimen with a crosshead rate of 1 mm min^{-1} by a universal testing machine (model 4482, Instron). During tensile loading, sensor signals are continuously sampled at 500 kHz by a DAQ (PCI-6110E, National Instrument) equipment to be stored in a personal computer. In addition, the reflective spectrum of the FBG sensor is monitored by an OSA (optical spectrum analyzer, model MS9710B, Anritsu). After the test, the stored signals are post-processed to produce the strain and damage signal. The output of the demodulator with a TFPF is processed to produce the strain of the FBG sensor at a sampling rate of 200 Hz equal to the driving frequency of the applied triangular wave. The output of the demodulator with a passive MZI is processed to produce the damage signal of the FBG sensor, which is compared with the piezoelectric sensor signal. A piezoelectric sensor signal is selected as a trigger source to capture the damage signals. The damage occurrence is considered as a surge in the piezoelectric sensor signal. At damage occurrence, damage signals passed through a digital high-pass filter with a cut-off frequency of 10 kHz were analyzed by the time-frequency analysis of a short-time Fourier transform.

3.2. Test results

Figure 6 shows the time-history of strains sampled at 200 Hz. The strain measured by an FBG sensor was almost the same as that measured by an ESG. The FBG sensor failed at 0.8%

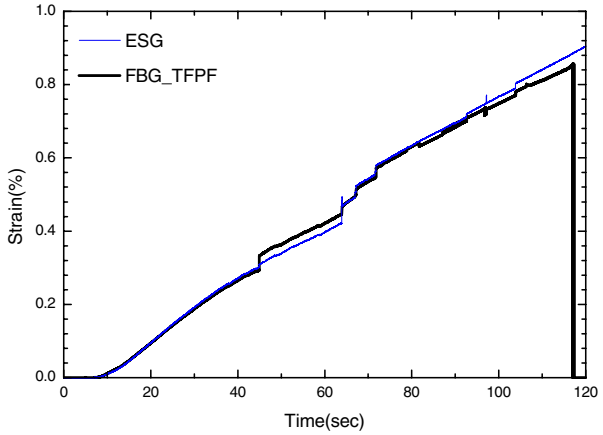

Figure 6. Strain in $[0_2/90_8]$ graphite/epoxy specimen sampled at 200 Hz.

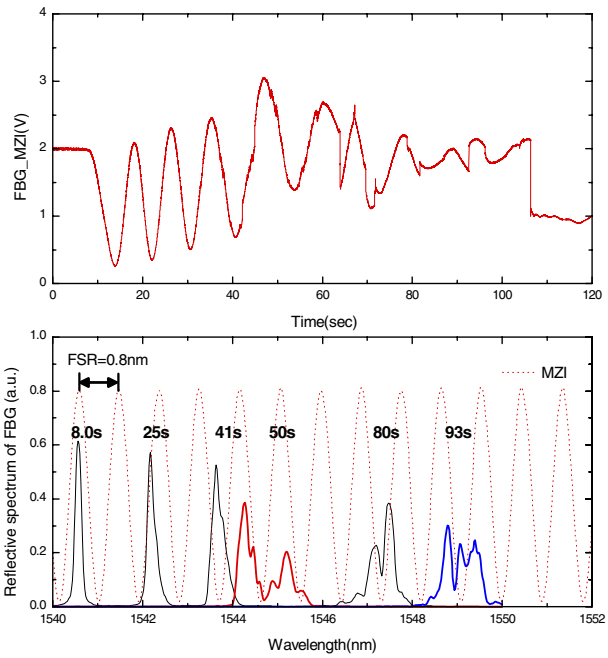

Figure 7. Output of a passive MZI demodulator and reflective spectrums of an FBG sensor.

of strain. In figure 7, the upper diagram shows the time-history of the output of the demodulator with a passive MZI sampled at 200 Hz and the lower one shows the evolutionary reflective spectrums of the FBG sensor. The initial output of the demodulator with a passive MZI showed a sinusoidal function of time. After about 0.4% of strain, it showed a weak sinusoidal function with time. The lower diagram showed that as the strain increased, the reflective bandwidth of the FBG sensor broadened to become wider than the FSR (∼0.8 nm) of MZI. It is well known that when an FBG is subject to a strain gradient or transverse strain, the reflective spectrum of the FBG broadens to have multiple Bragg wavelengths. Therefore, careful treatments including mounting and signal processing of an FBG sensor are required. In this paper, an averaged Bragg wavelength is used in the calculation of strain for the case of the split spectrum of the FBG.

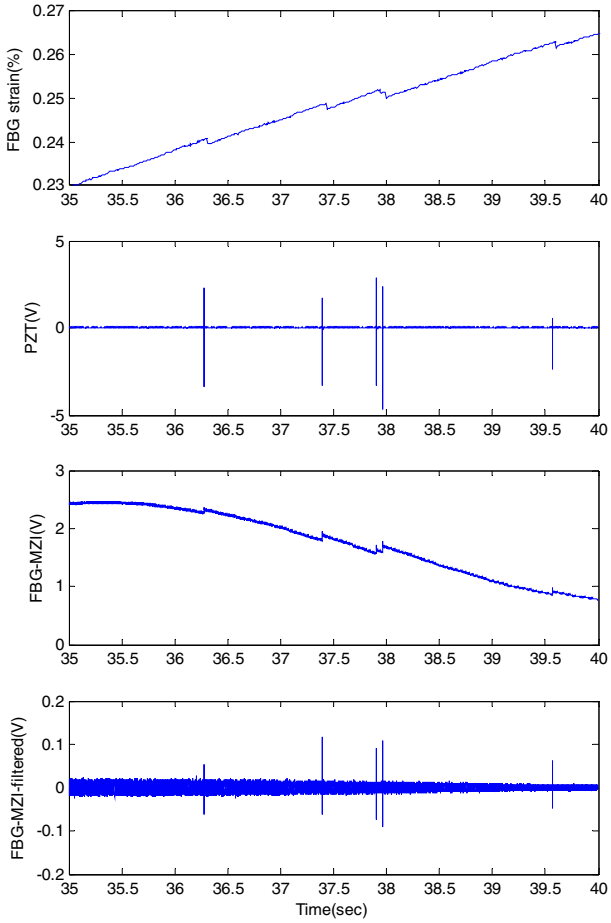

Figure 8. PZT signal, strain and high-frequency signal of FBG sensor between 35 and 40 s sampled at 500 kHz.

Figure 8 shows the sensor signals recorded between 35 and 40 s after loading, in which five damage events can be seen in the PZT signal. At each damage occurrence, a sudden strain shift was observed in the strain of the TFPF demodulator and a surge was also observed in the high-pass filtered signals of the demodulator with a passive MZI.

Figure 9 shows the enlarged signals detected by the PZT and the demodulator with a passive MZI at damage occurrence. The PZT signal contains frequency components ranging from 10 to 250 kHz. In the FBG sensor signal, frequency components ranging from 10 and 200 kHz were observed but the frequency intensity above 100 kHz seemed relatively weak.

An FBG sensor has less signal-to-noise ratio and less frequency bandwidth than the PZT sensor in acoustic emission detection for the following reasons. First, the broadband light source used in the FBG sensor system has a relatively higher noise level than a laser with single wavelength. Second, the photodetector employed in this FBG sensor system has a frequency bandwidth limit less than 200 kHz. Third, the sensitivity of an FBG with a long gauge length of 10 mm tends to be falling off at the high-frequency bandwidth with short wavelength of an ultrasonic wave, which needs further study.

Though the long gauge length of the FBG increases the chances of its spectrum being broadened or distorted, ultrasound detection is possible because the demodulator with

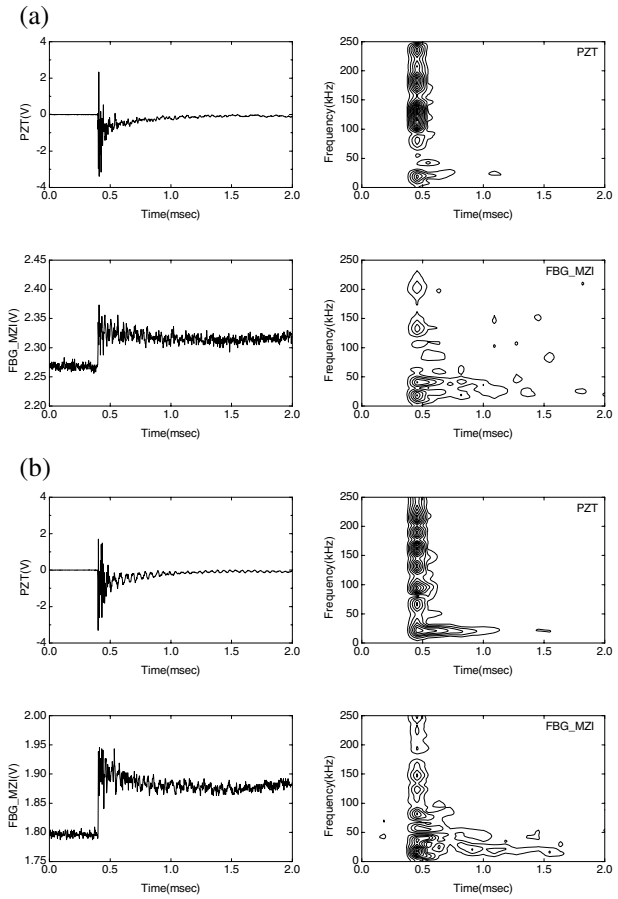

Figure 9. Damage signals and their frequency histories. (a) First damage ($t_{\text{origin}} = 36.277$ s), (b) second damage ($t_{\text{origin}} = 37.397$ s).

a passive MZI only detects the transmittance variation due to its spectrum shift. However, the distorted spectrum of the FBG results in low visibility of a passive MZI and low sensitivity of ultrasound detection. Therefore, a short gauge length of an FBG is recommended not only in the measurement of strain with gradient but also in acoustic emission detection.

The damage signal detected by the FBG sensor oscillated with DC voltage offset, which was coincident with a sudden strain shift. DC voltage offset was not observed in any damage signal detected by the PZT. This is because the PZT has low sensitivity to a quasi-static signal. It was inferred that dynamic strain release was generated at the transverse crack propagation in a 90° layer of a composite specimen. It is well known that multiple transverse cracking is formed by the increase of tensile load in cross-ply laminated composites and it can result in stiffness degradation [10]. Therefore, real-time monitoring of the damage signal would make it possible to predict residual stiffness of structures.

4. Conclusion

For the simultaneous measurement of strain and damage signal, an FBG sensor system with a dual demodulator is proposed. The dual demodulator is composed of one demodulator with a TFPF that can measure the low-frequency signal such as the strain and another with a passive MZI that can detect the high-frequency signal such as the damage or impact signal.

Using the proposed FBG sensor system, both the strain and the damage signals of a cross-ply laminated composite beam under tensile loading were simultaneously measured. The strain and the damage signals measured by the single FBG sensor showed that sudden strain shifts were accompanied with vibration at a maximum frequency of several hundred kilohertz at the instant of transverse crack propagation in the 90° layer of the composite beam. The DC voltage offset of the damage signal of the FBG sensor was coincident with a sudden strain shift, which could not be observed in damage signals detected by a piezoelectric sensor.

Therefore, the proposed FBG sensor system proved to have not only a wide measurement range but also high bandwidth and high sensitivity so that it can simultaneously measure various signals with different characteristics such as the strain and the damage signal, which could contribute to the minimization of the number of sensors required in structural health monitoring.

Acknowledgment

The authors appreciate the Agency for Defense Development, Korea, for financial support through Project ADD-03-05-02.

References

[1] Kwon I B, Kim C G and Hong C S 1997 Simultaneous sensing of the strain and failure instants of composite beams using fiber optic sensor *Compos. Sci. Technol.* **57** 1639–51

[2] Kim D H, Park J W, Kang H K, Hong C S and Kim C G 2002 Measuring dynamic strain of structures using a gold-deposited extrinsic Fabry–Perot interferometer *Smart Mater. Struct.* **11** 1–5

[3] Foedinger R, Rea D, Sirkis J, Troll J, Grande R and Vandiver T L 1999 Structural health monitoring and impact damage detection for filament wound composite pressure vessels *Proc. 2nd Int. Workshop on Structural Health Monitoring* pp 159–69

[4] Vohra S T *et al* 1997 Sixteen channel WDM fiber Bragg grating dynamic strain sensing system for composite panel slamming tests *12th OFS* pp 662–5

[5] Seim J M, Schulz W L, Udd E and Morrell M 1999 Higher speed demodulation of fiber grating sensors *Proc. SPIE* **3670** 8–15

[6] Perez I, Cui H L and Udd E 2001 Acoustic emission detection using fiber Bragg gratings *Proc. SPIE* **4328** 209–15

[7] Betz D C, Thursby G, Culshaw B and Staszewski W J 2003 Acousto-ultrasonic sensing using fiber Bragg grating *Smart Mater. Struct.* **12** 122–8

[8] Kersey A D, Berkoff T A and Morey W W 1993 Multiplexed fiber Bragg grating strain-sensor system with a fiber Fabry–Perot wavelength filter *Opt. Lett.* **18** 1370–2

[9] Kersey A D, Berkoff T A and Morey W W 1992 High-resolution fiber-grating based strain sensor with interferometric wavelength-shift detection *Electron. Lett.* **28** 236–8

[10] Lim S G and Hong C S 1989 Prediction of transverse cracking and stiffness reduction in cross-ply laminated composite *J. Compos. Mater.* **23** 695–713